Available online at www.sciencedirect.com

SciVerse ScienceDirect

Ceramics International 38 (2012) 4677–4684

CERAMICS INTERNATIONAL

www.elsevier.com/locate/ceramint

Acid-, base-, and heat-induced degradation behavior of Chinese sepiolite

Akira Miura [a,*], Koji Nakazawa [a], Takahiro Takei [a], Nobuhiro Kumada [a], Nobukazu Kinomura [a], Ryosaku Ohki [b], Hiroki Koshiyama [b]

[a] *Center for Crystal Science and Technology, University of Yamanashi, Japan*
[b] *Ask Technica Corporation, Japan*

Received 16 January 2012; received in revised form 11 February 2012; accepted 15 February 2012
Available online 7 March 2012

Abstract

The stability of Chinese sepiolite with respect to acid, base, and heat treatments was examined based on changes that occur in its crystal structure, its morphology, its surface area, and the ions that leach into solution. Treatment in HCl for 3 h caused predominantly Mg^{2+} to leach and increased the surface area of the sepiolite. Increased temperature accelerated the leaching, resulting in the disappearance of the sepiolite phase above 100 °C. Treatment in NaOH caused Si^{4+} to be leached and this was accompanied by a minor change in the crystal structure of the sepiolite. Thermal treatment in air caused the manifestation of several types of dehydration behavior and the sepiolite was decomposed completely at above ~800 °C. Composite sheets of sepiolite and nitrile butadiene rubber were made from sepiolite after it had undergone various treatments. The tensile stress of each composite was measured and this is discussed with respect to its degradation features.

Keywords: B. Composite; C. Mechanical properties; Sepiolite; Chemical treatment; Heat treatment

1. Introduction

Sepiolite is a natural, fibrous, phyllosilicate clay mineral with a high surface area and nano-sized channels. It is used in a number of applications including producing pharmaceuticals [1], filters [2], catalyst supports [3], absorbents [4,5], pigments [6,7], and sepiolite–polymer sheets [8,9]. It is also a candidate for asbestos substitutes [10,11] because of its less hazardous nature. Sepiolite is mined in Spain, Turkey, the USA, and China. Sepiolite mineral from China contains a larger fraction of long fibers [12], which offers advantages in terms of fabricating composite materials with better mechanical properties.

The theoretical formula of sepiolite is $Mg_8Si_{12}O_{30}(OH)_4(OH_2)_4{\cdot}nH_2O$. It consists of octahedrally coordinated magnesium layers and tetragonally coordinated silicon layers with nano-sized channels containing water [13,14], as shown in Fig. 1. According to previous reports, acid-, base- and heat-treatment of sepiolite alters its crystal structure and chemical composition [3,6,15–17]. Acid treatment of sepiolite removes Mg^{2+} located in its octahedral layer but leaves Si^{4+} coordinated in its tetrahedral layer [3]. In addition, acid attack greatly increases its surface area [3,15]. Base treatment causes a slight shift in its X-ray diffraction (XRD) peaks, but the reason for this is not clear [6,16]. Heat treatment causes dehydration below approximately 800 °C and induces a phase transition above 800 °C [6,17]. However, a systematic investigation of Chinese sepiolite has not been performed. In this report, the stability of Chinese sepiolite with respect to acid, base, and heat treatments is examined based on changes that occur in its crystal structure, its morphology, its surface area, and the ions that leach into solution. In addition, the mechanical properties of composites made of nitrile butadiene rubber (NBR) and sepiolite that had been treated with acid, base, and heat were measured. These investigations were performed because we believe that the durability of sepiolite produced from such treatments is important when considering its practical and potential applications. This is especially true for producing filter and sepiolite–polymer composites.

2. Experimental procedure

2.1. Chemical and heat treatments of sepiolite

Sepiolite of the composition shown in Table 1 was used as a starting material [18]. It contained calcite, dolomite, and quartz

* Corresponding author. Tel.: +81 055 220 8614; fax: +81 055 254 3035.
E-mail address: amiura@yamanashi.ac.jp (A. Miura).

0272-8842/$36.00
doi:10.1016/j.ceramint.2012.02.050

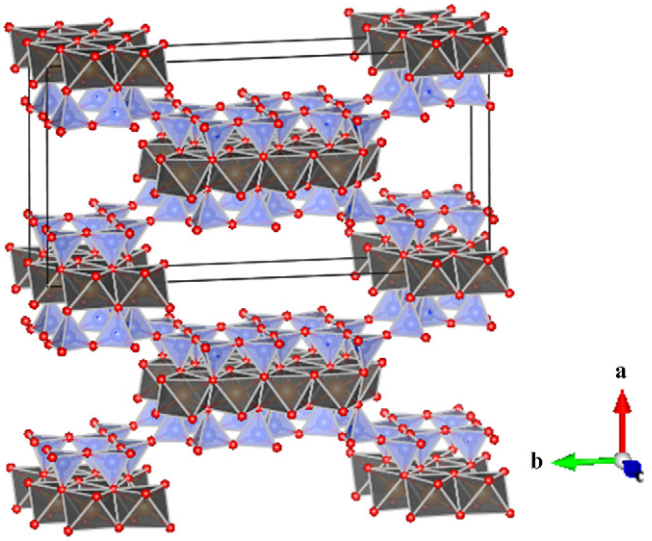

Fig. 1. The crystal structure of sepiolite. Mg–O octahedral layers are sandwiched in between Si–O tetragonal layers, thus forming nano channels along the *c*-axis. Zeolitic water in the nano channels is not drawn for the sake of brevity. The solid lines denote a unit cell.

impurities. First, sepiolite of ca. 60 g was dispersed in 2.0 L of a 1 mass% aqueous acetic acid and stirred for 48 h to remove the calcite. The powder was then filtered, rinsed with distilled water, and dried at 70 °C overnight. The sepiolite (0.60 g) was next put in a Teflon-lined steel autoclave together with 5 mass% aqueous HCl or 5 mass% aqueous NaOH (50 ml). Then, the autoclave was tightly closed and maintained at room temperature or kept in an oven that was operated at 40, 70, 100, 120 or 180 °C for 3–336 h. Afterward, each product was filtered, washed with distilled water, and dried at 70 °C for approximately 15 h. Heat-treated sepiolite was made by heating sepiolite without calcite at 300–900 °C at a rate of 1 °C/min and maintaining it at the maximum temperature for 1.5 h, after which the furnace was turned off.

2.2. Composite sheets of sepiolite and NBR

All of the composite sheets were produced using the same procedure [18], but they were made from the different types of sepiolite that were produced using the different treatments described above. Approximately 8.75 g of sepiolite was used to produce one sheet. Sepiolite powder was dispersed in 500 ml of water and ultra-sonicated at 28 kHz for 120 min. Following this, each solution was stirred with a magnetic stirrer for 5 min. Then, 3.75 g of NBR was added to each solution. To each of these was then added 25 ml of 1 M aqueous aluminum sulfate approximately 5 min after adding the NBR and stirred the mixtures for another 5 min. Then, each solution was deformed at 1500 rpm for 3 min. Sheets 150 mm in diameter were obtained by filtration using a suction pump for 30 min. Each sheet was compressed at a pressure of 10 MPa and dried at 50–70 °C for about 14 h.

Table 1
Chemical composition of Chinese sepiolite [18].

Composition	Mass%
SiO_2	36.8
MgO	16.5
CaO	19.4
Fe_2O_3	0.51
Al_2O_3	0.89
K_2O	0.10
Na_2O	0.11
lg. loss	25.3
Total	99.6

2.3. Characterization

Powder XRD (RINT-2000, Rigaku; CuKα radiation) was used for structural characterization. The specific Brunauer–Emmett–Teller (BET) surface area (S_{BET}) for each composite was derived from N_2 adsorption isotherms that were measured using a BELSORP-mini II (Bel Japan. Inc.). Scanning electron microscopy (SEM; JEOL 6300-F) was employed for making morphological observations of powder samples on carbon tape. The quantities of Ca^{2+}, Mg^{2+}, and Si^{4+} extracted from the sepiolite by the chemical treatments were determined by inductively coupled plasma-atomic emission spectroscopy (ICP-AES). The tensile stress of each composite was measured by using a universal testing instrument (A&D RTF-1325) at a pulling rate of 300 mm min^{-1}.

3. Results and discussion

3.1. Removal of calcite by acetic acid treatment

Sepiolite was characterized by XRD, SEM and N_2 adsorption before and after the acetic acid treatment. The XRD pattern of the starting material, shown in Fig. 2, exhibits the peaks assigned for sepiolite ($Mg_8Si_{12}O_{30}(OH)_4(OH_2)_4{\cdot}nH_2O$), calcite ($CaCO_3$), dolomite ($CaMg(CO_3)_2$), talc ($Mg_3Si_4O_{10}(OH)_2$), and quartz ($SiO_2$). The acetic acid treatment resulted in no significant difference without the

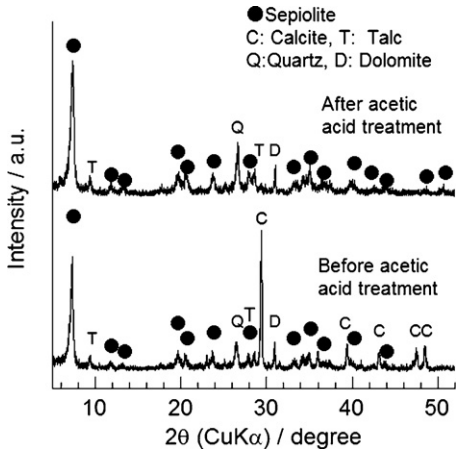

Fig. 2. XRD patterns of sepiolite before (downward) and after (upward) acetic acid treatment. ICSD patterns of sepiolite (#156199), calcite (#16710), talc (#21017), quartz (#34636), and dolomite (#10404) were used for the assignments.

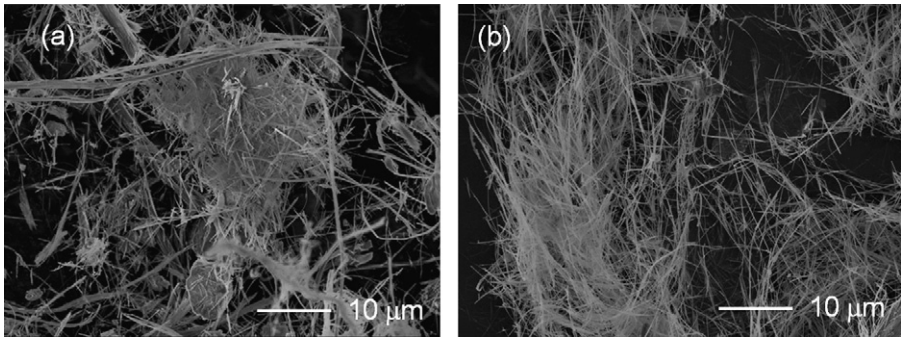

Fig. 3. SEM images of sepiolite (a) before and (b) after acetic acid treatment.

disappearance of the calcite peak. The amount of dissolved Ca^{2+} in solution was approximately 8 mass%, which was consistent with the removal of calcite phase. The quantities of dissolved Mg^{2+} and Si^{4+} were less than 0.6 mass%, implying that little or no compositional change in the sample occurred with respect to these elements.

Fig. 3 shows SEM images before and after the acetic acid treatment. Both the images show fibrous morphologies. The surface areas of the sepiolite before and after the treatment were 95.9 and 104 m^2/g, respectively. A slight increase in the surface area may be attributed to the removal of calcite with a relatively low surface area.

3.2. HCl treatment

HCl treatment was performed on the sepiolite after the removal of calcite by the acetic acid treatment as described above. Fig. 4 shows the relationship between the heating temperature and the quantities of ions that were leached from the samples into the 5 mass% HCl. With increasing temperature, the amount of Mg^{2+} increased, and a significant change was observed from 70 °C to 100 °C. If it is assumed that the removal of calcite from the sepiolite gives a single-phase theoretical dodecahydrate sepiolite ($Mg_8Si_{12}O_{30}(OH)_4(OH_2)_4{\cdot}8H_2O$), then 86% of Mg^{2+} in the sepiolite can be said to have dissolved at 120 °C. The amount of Ca^{2+} that was leached remained almost constant. An increase in the temperature also enhanced the leaching of Si^{4+} although the leached amount based on the theoretical sepiolite was only 5.3% at 120 °C. Thus, the products after HCl treatment were Si-rich in composition. The surface areas for the products are listed in Table 2. With increasing temperature up to 100 °C, the surface area increased. However, it decreased by further heating at 120 °C. Fig. 5 shows XRD patterns of the sepiolite before and after HCl acid treatment for 3 h at various temperatures. All of the treatments removed the dolomite peak, which is in agreement with the observed leaching of Ca^{2+} and Mg^{2+}. Above 100 °C, the sepiolite peaks changed to a very broad peak around 20–30°, which was related to the significant leaching of Mg^{2+}.

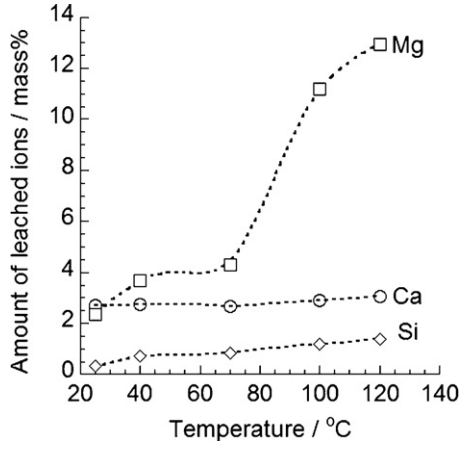

Fig. 4. Quantities of leached ions into HCl solution (5 mass%) by soaking sepiolite in an autoclave for 3 h at different temperatures.

The fibrous morphology of the sepiolite after the acid treatment can be seen at 70 and 120 °C in Fig. 6. At 120 °C, small amount of fibers longer than 10 μm were found.

According to the literatures [3,6,15], hydrochloric-, sulfuric-, or nitric-acid treatment at or below 80 °C leaches Mg^{2+} from sepiolite and forms micro-pores, thereby increasing the surface area of sepiolite. The leached amount increases with the soaking time, temperature, and concentration of the acid, and the sepiolite phase disappears over time. Our results show that a temperature of over 100 °C greatly enhanced the kinetics of Mg^{2+} leaching. The increase in surface area and the disappearance of sepiolite phase were observed at these temperatures.

3.3. NaOH treatment

The effect of NaOH treatment on the calcite deficient sepiolite was examined in terms of temperature and time. The base treatment leached predominantly Si^{4+}, but a small amount of Ca^{2+} was leached in addition to Mg^{2+} (less than 0.1 mass%),

Table 2
BET surface areas of sepiolite before and after HCl treatments for 3 h at various temperatures.

Treatment	S_{BET} (m^2/g)
Before	104
R.T.	166
40 °C	181
70 °C	227
100 °C	335
120 °C	197

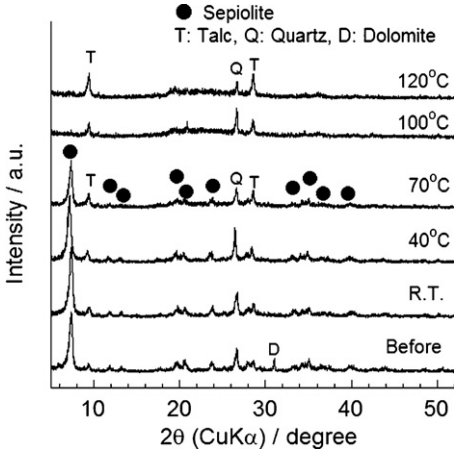

Fig. 5. XRD patterns of sepiolite before and after HCl treatment for 3 h at different temperatures. ICSD patterns of sepiolite (#156199), talc (#21017), quartz (#34636), and dolomite (#10404) were used for the assignments.

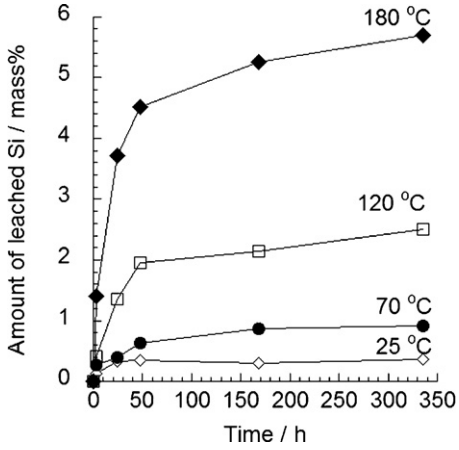

Fig. 7. Relationship between time and quantities of Si^{4+} leached into NaOH (5 mass%) by soaking sepiolite in an autoclave at different temperatures.

resulting in Mg^{2+}-rich products. The temperature dependence of the amount of Si^{4+} leached is shown in Fig. 7. With increasing temperature and time, the leached amount increased up to 5.7 mass%, which corresponds to 22% of Si^{4+} in the theoretical sepiolite. The leached rates decreased after 48 h of treatment. It was noted that the amount of leached Si^{4+} was less than that of Mg^{2+} by the acid treatment, indicating more tolerance of the sepiolite toward the base treatment. Table 3 shows that all of the treatments for 3 h resulted in comparable or slightly changed surface areas. While long-term treatment at room temperature did not cause any significant change, the treatments above 70 °C decreased the surface area.

The temperatures of the NaOH treatments altered the XRD patterns while the duration did not affect them significantly. Fig. 8 shows XRD patterns for before and after the NaOH treatments at various temperatures for 168 h. The pattern of the sepiolite after treatment at room temperature was similar to that before the treatment. In contrast, the diffraction peaks between 70–180 °C showed slightly different patterns. For example, the most intensive peak at 7.4° shifted toward a lower angle (7.0°) over the range 70–180 °C. The treatment at 180 °C resulted in another peak at 7.8°. Thus, NaOH treatment at above 70 °C likely caused structural changes in or decomposition of the sepiolite. The impurity phases of quartz and dolomite disappeared at 70 and 120 °C, respectively.

There were no significant differences in the SEM images after 3 h of treatment in the range between room temperature and 180 °C (Fig. 9(a)). It was possible to observe some fibers that were longer than 10 μm. On the other hand, the images of the sepiolite after 168 h for treatments at and above 70 °C showed decreased numbers of these fibers (Fig. 9(b)–(d)).

NaOH treatment for 3 h did not cause significant leaching at room temperature or at higher temperatures, indicating that the sepiolite was more tolerant toward the base treatment. However, long-term treatment at above 70 °C changed the composition, morphology, crystal structure, and surface area of the sepiolite. The morphological changes may be due to the crystallographic structural change of sepiolite and/or formation of Mg-rich compounds in the sepiolite after the leaching of the Si^{4+} ions. The origin of the change of crystal structure is not clear, although similar XRD patterns have been reported [6]. The decreased surface area can be explained by the partial destruction of nano-sized channels in the sepiolite, which were possibly related to the changes in its crystal structure or by the formation of Mg-rich compounds with low surface areas.

3.4. Thermal treatment

The decrease in weight of the sepiolite without calcite was measured by thermal gravimetric analysis (TGA; Fig. 10). The

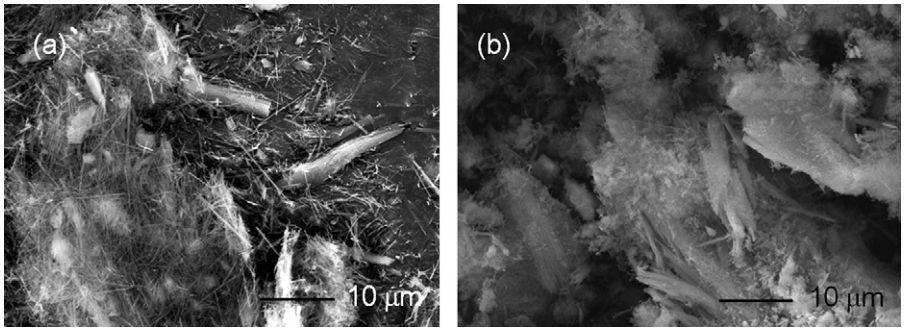

Fig. 6. SEM images of sepiolite after HCl treatment for 3 h at (a) 70 °C and (b) 120 °C.

Table 3
BET surface areas of sepiolite before and after NaOH treatment under various conditions.

Treatment	S_{BET} (m^2/g)
Before	104
25 °C/3 h	111
70 °C/3 h	97
120 °C/3 h	87
180 °C/3 h	112
25 °C/168 h	119
70 °C/168 h	56
120 °C/168 h	76
180 °C/168 h	61

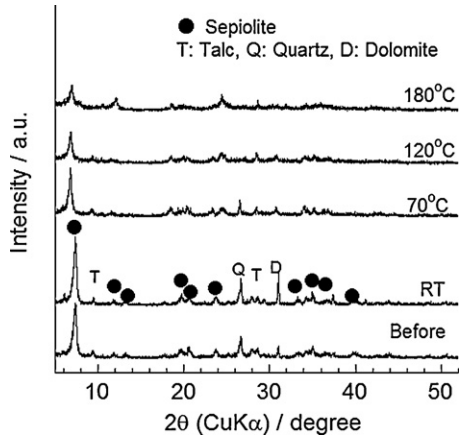

Fig. 8. XRD patterns of sepiolite before and after NaOH treatment for 168 h at different temperatures. ICSD patterns of sepiolite (#156199), talc (#21017), quartz (#34636), and dolomite (#10404) were used for the assignments.

mass of the sepiolite decreased rapidly at approximately 50 °C, 280 °C, 600 °C, and 800 °C, and was stable at above 900 °C.

The XRD patterns of the sepiolite after the different heat treatments are shown in Fig. 11. The pattern after the treatment at 300 °C was similar to that before the treatment. The patterns after the heat treatments over the range 450–750 °C had peaks that were assigned to sepiolite dihydrate, quartz, and talc. Peaks for clinoenstatite were observed after the heat treatment at 900 °C together with the peak for quartz. Similar fibers were observed at 450 and 900 °C (Fig. 12), although their lengths were shorter than those present before the treatments had been carried out. Table 4 shows that the surface area decreases with increasing treatment temperature.

The mass changes and phase changes were similar to those noted in previous reports [6]. The mass loss below and above approximately 300 °C corresponded to the loss of adsorbed water and water from the sepiolite framework (zeolitic water), respectively. The mass loss at around 800 °C was probably related to the phase transition changes from dehydrated sepiolite to clinoenstatite and was possibly accompanied by the formation of an amorphous phase. The decreased surface area may be caused by the destruction of nano-sized channels in sepiolite structure and the thermal aggregation of the fibers.

3.5. Mechanical properties of sepiolite–NBR composite sheets

We examined the mechanical properties of the composite sheets made from chemical/heat-treated sepiolite. Fig. 13 shows the relationship between the temperature for the HCl and NaOH treatments and the tensile strength of the sepiolite–NBR sheets, where the tensile stress of three pieces cut out from one

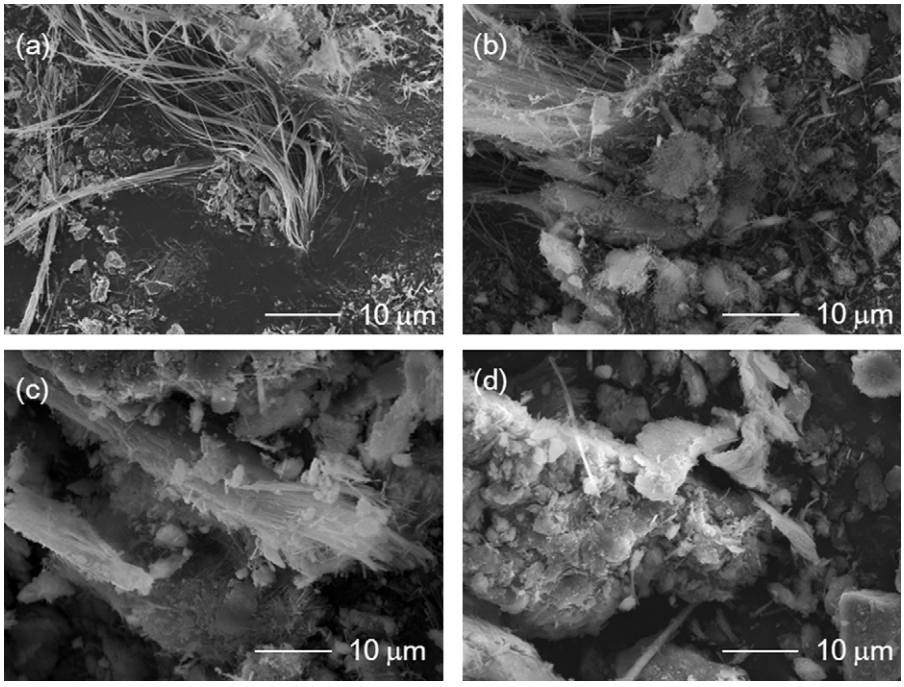

Fig. 9. SEM images of sepiolite after NaOH treatment (a) for 3 h at 180 °C and for 168 h at (b) 70 °C, (c) 120 °C, and (d) 180 °C.

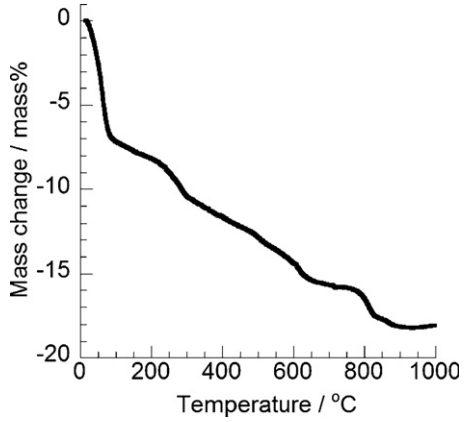

Fig. 10. A TG curve of sepiolite after acetic acid treatment in air at a heating rate of 10 °C/min.

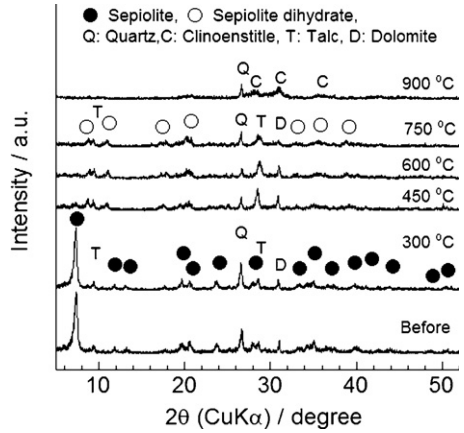

Fig. 11. XRD patterns of sepiolite before and after heat treatment for 3 h in air at different temperatures. ICSD patterns of sepiolite (#156199), sepiolite dihydrate (#156200), clinoenstatite (#30893), talc (#21017), quartz (#34636), and dolomite (#10404) were used for the assignments.

composite are plotted. The figure also details the strength of the sheets made from sepiolite that had only been treated with acetic acid. The tensile strengths of the sheets for the sepiolite that were only treated with acetic acid were greatest and ranged from 15.5 to 18.0. The HCl treatment greatly reduced their strengths to ~3 MPa even at room temperature. An increase in the temperature brought about further degradation. The NaOH treatment for 3 h reduced their strengths, but they displayed

Table 4
BET surface areas of sepiolite before and after heat treatment at different temperatures in air.

Treatment	S_{BET} (m^2/g)
Before	104
300 °C	95
450 °C	44
600 °C	44
750 °C	42
900 °C	8

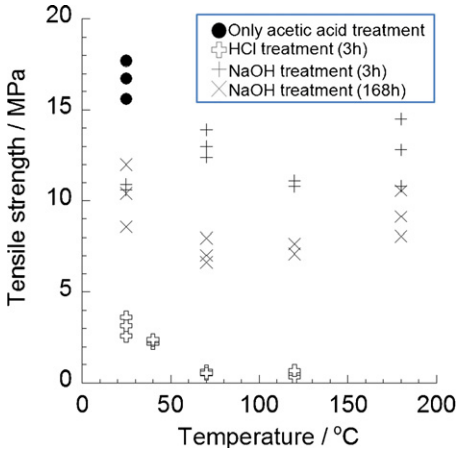

Fig. 13. Relationship between the tensile strength of sepiolite–NBR composite sheets and temperature for HCl and NaOH treatments. The sepiolite after these treatments was used as a component of each respective composite. The strength of three pieces cut out from one composite is plotted for the specific type of treatment noted in the figure.

much higher values when compared with that of the acid treated sheets. The treatments at different temperatures did not significantly affect their strengths. The sheets that underwent long-term treatment showed comparable or slightly decreased strengths independent of the temperature, indicating higher tolerances toward the base treatments.

Fig. 14 shows the relationship between the heating temperature and the tensile strength of the sepiolite–NBR sheets. The strength of the composite made from the sepiolite heated at 300 °C ranged from 6 to 9 MPa. These values are much higher than those of the composite made from acid-treated samples, which indicates that the intense acid degradation is not caused only by thermal degradation.

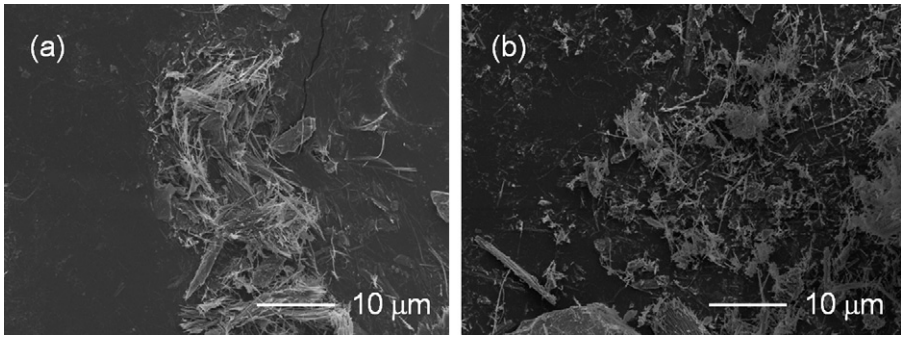

Fig. 12. SEM images of sepiolite before and after heat treatment for 3 h in air at (a) 450 °C and (b) 900 °C.

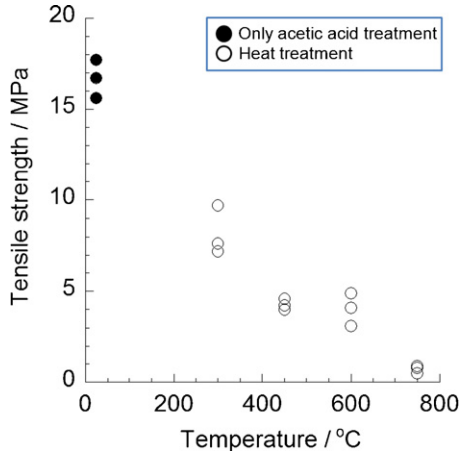

Fig. 14. Relationship between tensile strength of sepiolite–NBR composite sheets and temperature of for the heat treatment. Sepiolite after being heated at different temperatures was used as a component for each respective composite. The strength of three pieces cut out from one composite is plotted for the specific type of treatment in the figure.

Thermal treatment decreased their strengths with increasing temperature. The sheet that was produced from the sepiolite after treatment at 900 °C could not be fabricated because it could not be dispersed in water.

The strengths of the sheets may be related to the surface area of the sepiolite. Fig. 15 shows the relationship between the tensile strength and the surface area of the sepiolite after various treatments, where a peak at ∼110 m^2/g of the surface area can be seen. Thus, surface area measurement is considered useful for estimating the tensile strength of the composite. As described previously, the HCl treatment greatly increased the surface area of the sepiolite, while the NaOH and heat treatments increased or reduced it slightly. Thus, the degradation of strength caused by HCl treatment can be explained by the formation of micro-pores. In contrast, the base treatment did not bring about significant changes, possibly because of the absence of such micro-pores. The decreased strength caused by heat treatment possibly related

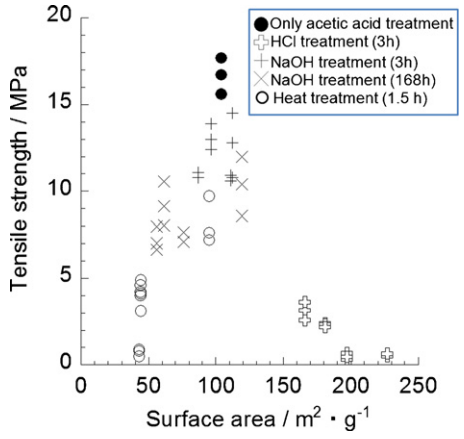

Fig. 15. Relationship between the tensile strength of sepiolite–NBR composite sheets and the surface area of the sepiolite. Sepiolite after various treatments was used as a component for each respective composite. The strength of three pieces cut out from one composite is plotted for the specific type of treatment noted in the figure.

to the structural changes that were accompanied by the decreased surface area. The possibility of other factors influencing the strength such as acetic acid-induced modifications to the surface cannot be precluded.

4. Conclusions

The degradation behavior of sepiolite was investigated following acid, base, and thermal treatments. Fibrous morphology was observed for all of the samples after the treatments, but smaller quantities of fibers were found in high-temperature or long-term treatment samples. While acid treatment intensively leached Mg^{2+} and caused an increase in the surface area of the sepiolite, base treatment caused moderate Si^{4+} leaching and decreased its surface area. Increases in temperature and time for both treatments brought about structural changes. Heat treatment in air caused dehydration, which was accompanied by structural changes and a decrease in the surface area of the sepiolite. The tensile strength of the sepiolite–NBR composites made from sepiolite after the treatments depended on the type of treatment that was carried out. The acid treatment brought about more severe degradation when compared with the base treatment and the thermal treatment in air below 300 °C.

Acknowledgement

We would like to acknowledge receiving financial support from NEDO (H.22: No. 073001) to carry out this work.

References

[1] M. Sugiura, M. Horii, H. Hayashi, M. Sasayama, Application of sepiolite to prevent bleeding and blooming for EPDM rubber composition, Appl. Clay Sci. 11 (2–4) (1996) 89–97.
[2] M.R. Weir, E. Rutinduka, C. Detellier, C.Y. Feng, Q. Wang, T. Matsuura, R. Le Van Mao, Fabrication, characterization and preliminary testing of all-inorganic ultrafiltration membranes composed entirely of a naturally occurring sepiolite clay mineral, J. Membr. Sci. 182 (1–2) (2001) 41–50.
[3] A.J. Aznar, E. Gutiérrez, P. Díaz, A. Alvarez, G. Poncelet, Silica from sepiolite: preparation, textural properties, and use as support to catalysts, Microporous Mater. 6 (2) (1996) 105–114.
[4] A. Kilislioglu, G. Aras, Adsorption of uranium from aqueous solution on heat and acid treated sepiolites, Appl. Radiat. Isot. 68 (10) (2010) 2016–2019.
[5] A. Rodríguez, G. Ovejero, M. Mestanza, J. García, Removal of dyes from wastewaters by adsorption on sepiolite and pansil, Ind. Eng. Chem. Res. 49 (7) (2010) 3207–3216.
[6] R. Giustetto, O. Wahyudi, I. Corazzari, F. Turci, Chemical stability and dehydration behavior of a sepiolite/indigo Maya Blue pigment, Appl. Clay Sci. 52 (1–2) (2011) 41–50.
[7] B. Hubbard, W. Kuang, A. Moser, G.A. Facey, C. Detellier, Structural study of Maya Blue: textural, thermal and solid state multinuclear magnetic resonance characterization of the palygorskite–indigo and sepiolite–indigo adducts, Clays Clay Miner. 51 (2003) 318–326.
[8] L.I. Rueda, C.C. Antón, M.C.T. Rodriguez, Mechanics of short fibers in filled styrene–butadiene rubber (SBR) composites, Polym. Compos. 9 (3) (1988) 198–203.
[9] L. Bokobza, J.-P. Chauvin, Reinforcement of natural rubber: use of in situ generated silicas and nanofibres of sepiolite, Polymer 46 (12) (2005) 4144–4151.
[10] H. Noda, K. Miyagawa, M. Kobayashi, H. Horiguchi, K. Ozawa, N. Kumada, Y. Yonesaki, T. Takei, N. Kinomura, Preparation of cordierite

from fibrous sepiolite, J. Ceram. Soc. Jpn. 117 (1371) (2009) 1236–1239.
[11] N. Kumada, Y. Yonesaki, T. Takei, N. Kinomura, M. Kobayashi, H. Horiguchi, Hydrothermal conversion of chrysotile to amorphous silica or brucite, J. Ceram. Soc. Jpn. 117 (1371) (2009) 1240–1242.
[12] B. Bellmann, H. Muhle, H. Ernst, Investigations on health-related properties of two sepiolite samples, Environ. Health Perspect. 105 (Suppl. 5) (1997) 1049–1052.
[13] K. Brauner, A. Preisinger, Struktur und entstehung des sepioliths, Miner. Petrol. 6 (1) (1956) 120–140.
[14] J.E. Post, D.L. Bish, P.J. Heaney, Synchrotron powder X-ray diffraction study of the structure and dehydration behavior of sepiolite, Am. Mineral. 92 (1) (2007) 91–97.
[15] M.A.V. Rodriguez, J.de D. Lopez Gonzalez, M.A.B. Munoz, Influence of the free silica generated during acid activation of a sepiolite on the adsorbent and textural properties of the resulting solids, J. Mater. Chem. 5 (1) (1995) 127–132.
[16] D.C. Golden, J.B. Dixon, H. Shadfan, L.A. Kippenberger, Palygorskite and sepiolite alteration to smectite under alkaline conditions, Clays Clay Miner. 33 (1) (1985) 44–50.
[17] R.L. Frost, J. Kristóf, E. Horváth, Controlled rate thermal analysis of sepiolite, J. Therm. Anal. Calorim. 98 (3) (2009) 749–755.
[18] H. Noda, K. Miyagawa, T. Takei, Y. Yonesaki, N. Kumada, N. Kinomiura, M. Kobayashi, H. Horiguchi, Temperature gradient in an inorganic insulator from change of mineral phases by heating, J. Soc. Inorg. Mater. Jpn. 16 (2009) 89–93.